Opportunities and Limitations in Broadband Sensing

Anthony M. Polloreno,[1] Jacob L. Beckey,[1] Joshua Levin,[1,2] Ariel Shlosberg,[1]
James K. Thompson,[1] Michael Foss-Feig,[2] David Hayes,[2] and Graeme Smith[1]

[1]*JILA, NIST and University of Colorado, Boulder, Colorado 80309, USA*
[2]*Quantinuum, 303 S. Technology Ct., Broomfield, Colorado 80021, USA*

We consider estimating the magnitude of a monochromatic AC signal that couples to a two-level sensor. For any detection protocol, the precision achieved depends on the signal's frequency and can be quantified by the quantum Fisher information. To study limitations in broadband sensing, we introduce the integrated quantum Fisher information and derive inequality bounds that embody fundamental tradeoffs in any sensing protocol. These inequalities show that sensitivity in one frequency range must come at a cost of reduced sensitivity elsewhere. For many protocols, including those with small phase accumulation and those consisting of π-pulses, we find the integrated Fisher information scales linearly with T. We also find protocols with substantial phase accumulation can have integrated QFI that grows quadratically with T, which is optimal. These protocols may allow the very rapid detection of a signal with unknown frequency over a very wide bandwidth.

Introduction—Quantum systems such as atoms are naturally good sensors because they are identical and their environments can be well-controlled experimentally. The detection of weak signals requires the consideration of quantum effects, and entangled detectors are well-known to be more sensitive than their unentangled counterparts [1]. Indeed, by using techniques like squeezing, quantum sensors have been used for dark matter searches, entanglement enhanced magnetometry, microwave clocks, and matterwave interforemeters. [2–11].

Quantum Fisher information (QFI) quantifies the performance of a parameter estimation protocol [12]. For a pure state $\rho_\theta := |\psi_\theta\rangle\langle\psi_\theta|$, parameterized by θ, the QFI is

$$J(\theta) = 2\mathrm{Tr}\left[(\partial_\theta \rho_\theta)^2\right], \tag{1}$$

[13]. The QFI tells us, via the Cramer-Rao bound [14], how well an unbiased estimator of θ can approximate its true value. In particular, given m copies of $|\psi_\theta\rangle$ the variance of any unbiased estimator $\hat{\theta}$ must satisfy $\mathrm{Var}(\hat{\theta}) \geqslant \frac{1}{mJ(\theta)}$. Furthermore, this bound can be saturated, so the more Fisher information a protocol has, the better you can estimate θ.

We consider estimating the strength of a time-varying signal at frequency ω using a qubit that couples to the signal according to

$$H(t) = \mu B \cos(\omega t + \varphi) Z, \tag{2}$$

where μ is the magnetic moment of the qubit. For instance, we may wish to estimate the strength of an AC magnetic field [15–23]. While we have included φ in the analysis in Eq. 7, we have omitted it for convenience elsewhere. In general, φ changes the peak of the sensitivity, and averaging over and unknown φ only affects our results by a multiplicative constant. This is the case that is relevant, for instance, to axion searches where the phase of the signal is not known. To gather information about this Hamiltonian, we need to establish a protocol, which generically consists of preparing the sensing qubit in an initial state, applying a time-dependent control sequence, and finally performing a measurement. The performance of a protocol will depend on the frequency of the signal ω. For example, preparing $|+\rangle$ followed by free evolution for time T and measurement in the $|\pm\rangle$ basis is optimal for $\omega = 0$ but performs poorly for $\omega \gg 1/T$. In fact, we will show that trade-offs in sensitivity at different frequencies are inevitable. We make this quantitative by considering the integrated QFI (IQFI). In general, a choice of protocol includes a choice of measurement basis, as defined above. In the majority of examples we consider in this paper, the optimal measurement basis is frequency independent, so that the the optimization over the final POVM in the definition of QFI can be ignored. For this reason, in this paper we consider integrating the QFI over all frequencies. While this is different than the integrated sensitivity of a single protocol, it provides an analytically tractable method of analysis which is tight in many cases of interest, namely weak fields and protocols consisting only of $\pi-$pusles. By bounding this integral we formalize the idea that there is a fundamental tension between having sensitivity in different frequency bands.

The longer we observe a signal, the more we can expect to know about it. Thus, it is no surprise that the IQFI will typically grow with the duration T of a protocol. In fact, we find a number of constraints on how IQFI grows with T. First, we find that any protocol starting on the equator of the Bloch sphere that involves only π-pulses has an IQFI of $2\pi\zeta^2 T$, where $\zeta \equiv \mu/\hbar$ is the inverse gyromagnetic ratio of the system being used as a sensor [24]. Second, for an arbitrary protocol with $\zeta BT/ \ll 1$, the IQFI is close to $2\pi\zeta^2 T$. Then we find a particular protocol that significantly exceeds $2\pi\zeta^2 T$ — by continuously transversely driving a spin with a gX term, our protocol has a peak sensitivity around $2g$, with IQFI scaling quadratically with time. We further show that the IQFI can not exceed quadratic scaling with time, so that this protocol is in a sense optimal. However, the practical restriction to the small signal regime $\zeta BT \ll 1$ is not uncommon, due in part to phase ambiguities that may arise in the accrued phase if one begins to violate this limit. Additionally if T_d is a characteristic decoherence time of the system, then we are practically constrained to $T < T_d$. Thus for $B \ll 1/(\zeta T_d)$ and fixed T_d, we also find $\zeta BT \ll 1$. In these contexts, our result show that sensing should be expected to be limited by the bound of $2\pi\zeta^2 T$. Physically, this corresponds to when the peak angular excursion of the Bloch vector is much less than π. On the other hand, for weak fields, if we can sense for long times so that $\zeta BT \not\ll 1$, then we can accumulate quadratically more IQFI.

Beyond signal estimation and detection, our results can be applied to better understand the performance of dynamical decoupling [25–28]. Here we find that for many protocols, the average (over the initial state) IQFI is at least linearly proportional to T. As a result, dynamical decoupling can at best move the noise sensitivity of a qubit around in frequency space, rather than eliminating sensitivity at all frequencies. This gives a firm grounding to the intuition provided in [29] that considers the filter functions associated with CPMG sequences [30–32].

We note that the setting under consideration is different from the waveform estimation studied in [33]. That work studied how to simultaneously estimate a large number of parameters representing the full time series of a waveform. We consider the sensing problem of estimating a single Fourier amplitude, i.e. the systems we consider couple to a monochromatic signal $B\cos(\omega t)$. The relative simplicity of this setting admits a global analysis of the performance of an arbitrary protocol at different frequencies.

Preliminaries—We will consider Hamiltonians of the form Eq. (2), motivated by a spin-$\frac{1}{2}$ particle in a magnetic field. We first consider estimation protocols composed of instantaneous, arbitrary unitary rotations P_i followed by periods of free evolution. The choice of measurement at the end of the protocol is assumed to be optimal in the sense that it maximizes the Fisher information of the resulting classical probability distribution. So, for a state starting in the $+1$ X eigenstate, we have the final state

$$|\psi(T,\omega)\rangle = U_{N-1}P_{N-1}(t_N,t_{N-1})\ldots U_0(t_1,t_0)P_0|+\rangle, \quad (3)$$

where $t_N = T$ and $U(t_{i+1},t_i)$ is the time evolution operator under the Hamiltonian in Eq. 2 between times t_i and t_{i+1}. Specifically, $U(t_{i+1},t_i) = \exp\left(-\frac{i}{\hbar}\int_{t_i}^{t_{i+1}} H(t)dt\right) = \exp\left(-i\zeta B\Theta(t_{i+1},t_i)Z\right)$, where $\Theta(t_{i+1},t_i) = (\sin(\omega t_{i+1}+\varphi)) - \sin(\omega t_i+\varphi))/\omega$.

Given Eq. 3, the quantum Fisher information $J(B) = 2\mathrm{Tr}((\partial_B\rho_B)^2)$ tells us how well we can estimate B. We write $J(B|\omega)$ to indicate that Fisher information with respect to B will in fact depend on the signal frequency ω. Writing

$$|\phi_B\rangle := \partial_B|\psi_B\rangle = \quad (4)$$
$$-i\zeta\sum_{i=0}^{N}\Theta(t_{i+1},t_i)N-1\ldots ZU_iP_i\ldots U_0P_0|+\rangle,$$

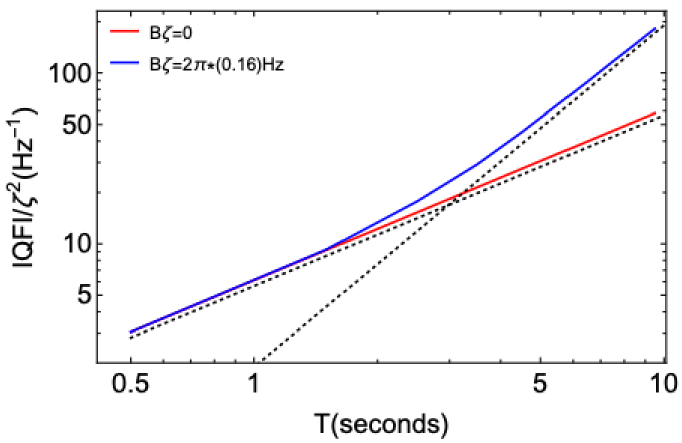

FIG. 1: Integrated IQFI for using $X_{\pi/2}$ pulses. Depending on the magnetic field strength we observe a more rapid accumulation of IQFI. The dashed lines are $\sim T$ and $\sim T^2$ scalings to guide the eye. For non-zero magnetic field, we see that a crossover from quadratic to linear scaling occurs when when $BT\zeta \ll 1$ (where the perturbative results are valid).

we find that the QFI can be expressed [13, 34]

$$J(B|\omega) = 4(\langle\phi|\phi\rangle + \mathrm{Re}\{\langle\phi|\psi\rangle^2\}), \quad (5)$$

where we have left the dependence on B implicit. Now, to understand the total sensitivity of a protocol across all frequencies we define the integrated QFI (IQFI) for a protocol with total evolution time T as [35]

$$K(T) = \int_0^\infty d\omega J(B|\omega). \quad (6)$$

Ramsey and π-pulse protocols—Within the family of control sequences consisting of instantaneous rotations interleaved with free-evolution, we now consider Ramsey spectroscopy, where a qubit is prepared on the equator of the Bloch sphere and allowed to freely precess. Here Eq. 4 becomes $|\phi\rangle = -i\zeta\Theta(T,0)|\psi\rangle$ and Eq. 5 gives $J(B|\omega) = 4\zeta^2\Theta^2(T,0)$. Defining $\zeta \equiv \mu/\hbar$, the IQFI follows as

$$K(T) = 4\zeta^2\int_0^\infty d\omega\frac{(\sin(\omega t+\varphi) - \sin(\varphi))^2}{\omega^2}, \quad (7)$$
$$= 2\zeta^2 T(\pi - \ln(4)\sin(2\varphi)). \quad (8)$$

If φ is unknown and therefore random in each experiment, averaging over φ gives $K(T) = 2\pi\zeta^2 T$, but if φ is known and we wish to maximize the IQFI, we would lock the experimental sequence to $\varphi = 3\pi/4$ to get $K(T) = 2\zeta^2 T(\pi + \ln 4)$. For convenience, in what follows we assume $\varphi = 0$, but note that averaging over φ should be possible in principle.

Now consider a protocol applying π-pulses at times $t_1,\ldots,t_N = T$. At time t_i we apply either X, Y or Z.

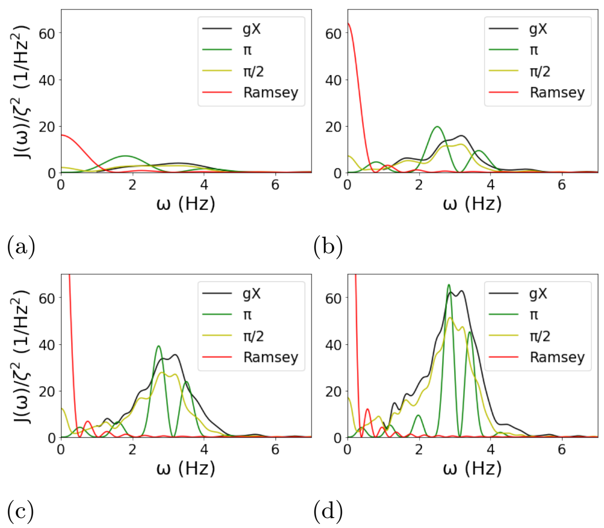

FIG. 2: QFI as a function of frequency for some protocols considered in this paper, for different protocol times T [(a) $T = 2$, (b) $T = 4$, (c) $T = 6$, and (d) $T = 8$ seconds], with $B\zeta = 1$ Hz. Ramsey has a large DC QFI, as expected, and very little ability to detect any AC signal. π-pulses, on the other hand, can be used to measure signals at higher frequencies, as might be expected from spectroscopy techniques such as CPMG. The gX protocol, with $g = 2\pi \times \frac{1}{4}$Hz in this example, is seen to be sensitive near $2g$. Moreover, it is seen to be sensitive over a broad bandwidth. The π-protocol shown here consists of π rotations about the X axis, at each integer value of time. The $\pi/2$-protocol consists of $\pi/2$ rotations about the X axis, every half second. Similar to the π-protocol, the $\pi/2$-protocol has AC sensitivity, as well as more broadband sensitivity.

Additionally, we can apply any unitary that leaves the expectation value of Z invariant. Then we have

$$K(T) = 4\zeta^2 \int_0^\infty d\omega (\sum_{i=0}^{N-1} \Theta(t_{i+1}, t_i))^2 \tag{9}$$

Using $\int_0^\infty \sin(\omega t_1)\sin(\omega t_0)/\omega^2 d\omega = \frac{\pi}{2}\min(t_1, t_0)$, we see for $t_3 \geqslant t_2 \geqslant t_1 \geqslant t_0$ that $\int_0^\infty d\omega \Theta_\omega(t_3, t_2)\Theta_\omega(t_1, t_0) = 0$. Thus Eq. (9) gives

$$K(T) = 2\pi\zeta^2 T. \tag{10}$$

$$\int d\mu K(T) = \frac{4\pi\zeta^2 T}{3}, \tag{11}$$

where μ is the Haar measure.

This average has important implications for dynamical decoupling protocols based on π-pulses. It shows that for such protocols a qubit must maintain a sensitivity to environmental noise over a substantial frequency range. Indeed, in the presence of white noise any π-pulse protocol will leave the qubit equally degraded by the noise. Specifically, we imagine that a qubit is subjected to a background power spectrum of magnetic field noise fluctuations whose noise spectrum is flat. A lower bound on the IQFI implies a lower bound on how much of this noise spectrum the qubit will experience, and therefore on its decoherence. For noise with more structure, these protocols do not allow sensitivity to noise to be eliminated, but can simply move that sensitivity to a frequency range where the environmental noise is fairly low.

B=0 Bound—We now present an argument to bound $K(T)$ at $B = 0$, and approximately bound $K(T)$ for short times and weak magnetic fields. Consider protocols with a control Hamiltonian $H_0(t)$ in addition to the signal Hamiltonian $H(t)$. We can then write $|\psi(T)\rangle = U\mathcal{U}|\psi_0\rangle$, where U is the time evolution due to H_0 and $\mathcal{U}$ is the interaction picture time-evolution, given by

$$\mathcal{U} = 1 - i\zeta B \int_0^t \cos(\omega\tau) Z_I(\tau) d\tau + O(B^2), \tag{12}$$

where we have used $Z_I(t)$ to express Z in the interaction picture. Then we have

$$|\phi\rangle_0 := \partial_B |\psi(t)\rangle\Big|_{B=0} = -i\zeta U \int_0^t \cos(\omega\tau) Z_I(\tau) d\tau |\psi_0\rangle. \tag{13}$$

Substituting into Eq. 5 and integrating, we find that the IQFI is at most $2\pi\zeta^2 T$. For small B and T, the next term on dimensional grounds should be $\mathcal{O}(B^2T^3)$, since we can show the term linear in B is zero. This dimensional analysis assumes that there are no other dimensionful quantities - for instance, if the interpulse spacings are not functions of T, then there may be other terms. Thus we find

$$K(T) \leqslant 2\pi\zeta^2 T + O(\zeta^4 B^2 T^3) \tag{14}$$

The full proof is provided in Appendix D. This shows that for small magnetic fields and short times we should expect a roughly linear scaling of the IQFI.

Entangled probe advantage— From standard results [36, 37] we expect that entangled inputs can outperform this bound. Indeed, consider an $n-$qubit GHZ state

$$|GHZ\rangle_n = \frac{1}{\sqrt{2}}(|0\rangle^{\otimes n} + |1\rangle^{\otimes n}). \tag{15}$$

This state accumulates phase as

$$U(t_{i+1}, t_i)^{\otimes n}|GHZ\rangle_n \tag{16}$$

$$= \frac{1}{2}(e^{iBn\Theta(t_{i+1},t_i)}|0\rangle^{\otimes n} + e^{-iBn\Theta(t_{i+1},t_i)}|1\rangle^{\otimes n}), \tag{17}$$

so that an analogous argument gives an IQFI at $B = 0$ of

$$K(T) = 2\pi n^2 \zeta^2 T. \tag{18}$$

Conversely, product input states can be reduced to the single qubit example, since $J(\rho^{\otimes n}) = nJ(\rho)$, so that for

n qubits starting in a product state, again with $B = 0$, we have

$$K(T) \leqslant 2\pi n\zeta^2 T. \tag{19}$$

So, while entanglement allows us to increase the coefficient in front of T, IQFI still increases linearly with time.

Quadratic scaling of IQFI— We have seen that π-pulse protocols and protocols with $BT\zeta \ll 1$ have IQFI that scales no faster than $2\pi\zeta^2 T$. Even an entanglement-enhanced protocol gives linear scaling of IQFI with T, albeit with an improved coefficient. While it is tempting to think linear scaling is optimal, we now give a simple protocol with IQFI scaling quadratically in T.

We consider a continuous-time protocol which applies a transverse field, $\hbar gX$, to the sensing qubit. This gives a full Hamiltonian of

$$H(T) = \hbar gX + \mu B\cos(\omega T)Z. \tag{20}$$

Assuming $\omega \sim 2g$, $BT\zeta \gg 1$ and using the rotating wave approximation [38], we find

$$J(B|\omega) \sim \frac{(\zeta T)^2}{(1+(\frac{\omega-2g}{B\zeta})^2)^2} \tag{21}$$

which we can integrate from $\omega = g$ to $\omega = 3g$ to get a lower bound of

$$K(T) \gtrsim \zeta^2 T^2\left(\frac{g}{1+\frac{g^2}{\zeta^2 B^2}} + \zeta B\tan^{-1}\left(\frac{g}{\zeta B}\right)\right). \tag{22}$$

Representative dynamics in this regime are shown in Fig. 3 and 4 of [39].

This protocol can be approximated by a discrete pulse-based protocol, described by Eq. 3 and given by Trotterization, that intersperses instantaneous rotations around the X-axis by periods of free evolution under the magnetic field. For times T, we can approximate evolution under Eq. 20 by m periods of free evolution of duration $\frac{T}{m}$ separated by rotations of angle $\frac{T\pi}{m}$ about the X-axis. Indeed, in Fig. 1, we see quadratic scaling choosing $m = 2T$. In Fig. 2 we compare the QFI of the $m = T$ and $m = 2T$ cases with the gX protocol and a Ramsey protocol, where it is evident that both the $m = 2T$ protocol and the gX protocol accumulate IQFI more rapidly than the other two protocols. These discrete protocols with quadratic scaling of IQFI have the property that the number of pulses scales with the total time of the protocol. In fact, this is necessary, as we will now see.

Consider a protocol with N pulses P_i applied between periods of free evolution U_i. Because $\langle\psi|\psi\rangle = 1$, $\partial_B\langle\psi|\psi\rangle = 0$, we have $\langle\phi|\psi\rangle = -\langle\psi|\phi\rangle$. This means that $Re(\langle\phi|\psi\rangle) = 0$, and so $\langle\psi|\phi\rangle^2$ has real part that is non-positive. Thus from Eq. 5 we see

$$J(B|\omega) \leqslant 4\langle\phi|\phi\rangle. \tag{23}$$

Now define $V_{ij} = \langle +|P_1^\dagger U_1^\dagger ... P_i^\dagger Z U_i^\dagger ... P_N^\dagger U_N^\dagger U_N P_N ... U_j Z P_j ... U_1 P_1|+\rangle$, then we see that $\langle\phi|\phi\rangle = \zeta^2\sum_{i,j}^N \Theta_i\Theta_j V_{ij} = \zeta^2\mathbf{\Theta}^T V\mathbf{\Theta}$, where $\mathbf{\Theta}$ is a vector whose i^{th} entry is Θ_i. V is an $N\times N$ complex matrix with entries of norm at most 1, so its eigenvalues have norm at most N. We thus find

$$K(T) = \int_0^\infty d\omega J(\omega) \leqslant 4\int_0^\infty d\omega\langle\phi|\phi\rangle \tag{24}$$

$$= 4\zeta^2\int_0^\infty d\omega\mathbf{\Theta}^T V\mathbf{\Theta} \tag{25}$$

$$\leqslant 4\zeta^2\int_0^\infty d\omega N|\mathbf{\Theta}|^2 = 2\pi N\zeta^2 T. \tag{26}$$

In order to have quadratic scaling in T, we must have a number of pulses N that scales linearly with T.

We will now see that the bound Eq. (24) can be used to show that the IQFI can scale at most quadratically with time, so that up to a constant the IQFI of the gX protocol scales as fast as possible.

A continuous-time protocol involves a control Hamiltonian G that gives a total Hamiltonian of the system

$$H(t) = \hbar G(t) + \mu B\cos(\omega t)Z. \tag{27}$$

We can Trotterize this evolution into a discrete sequence [40] like those considered in proving Eq. (24), with some inter-pulse duration δt. To zeroth order, the evolution will be

$$U'(T) = \mathcal{T}e^{i\int_{(N-1)\delta t}^{N\delta t} dtG(t)}e^{i\zeta B\Theta_N Z}...\mathcal{T}e^{i\int_0^{\delta t} dtG(t)}e^{i\zeta B\Theta_1 Z} \tag{28}$$

with $N\delta t = T$. We use $\mathcal{T}$ to denote a time-ordering, since $G(t)$ will not in general commute with $G(t')$ at $t' \neq t$.

By linearity of the derivative we can constrain the derivative of the Trotterized evolution to be close to the actual derivative. Using $U(t)$ to refer to the continuous time protocol, and $\hat{\epsilon}''(t)$ to refer to the error between the $\partial_B(U(t))$ and $\partial_B(U'(t))$, we see from Eq. (23),

$$J(\omega) \leqslant J_d(\omega) + \\ 8Re(\langle +|\hat{\epsilon}''(T)^\dagger\partial_B U'(T)|+\rangle) + 4\langle +|\hat{\epsilon}''(T)^\dagger\hat{\epsilon}''(T)|+\rangle),$$

where we've used $J_d(\omega)$ to denote the QFI of the protocol given by $U'(t)$. We can bound the integral of these terms by splitting the integral into two parts, one up to a frequency Ω and bounding by a constant, and the second by considering the explicit form of the Trotter error presented in [41], and expanding in $1/\omega$. Ultimately, as show in Appendix C, this gives a bound of

$$K(T) \leqslant \frac{2\pi\zeta^2 T^2}{\delta t} + (c(\delta t, \Omega, \mu B, \hbar||G||) \\ + \epsilon(\delta t, \Omega, \mu B, \hbar||G||))T^2, \tag{29}$$

where $||G||$ is maximum spectral norm of the control, $\max_{t\leqslant T}||G(t)||$ and c and ϵ are functions that control the error in approximating the IQFI of the continuous protocol by the IQFI of the Trotterization. This proves that $K(T) \in \mathcal{O}(T^2)$. Thus, our examples with quadratic scaling are asymptotically optimal in the amount of IQFI they accumulate.

Conclusions— The QFI provides an ultimate bound on how well a quantity can be estimated, in our case the amplitude of a sinusoid with fixed frequency. Integrating the QFI over all frequencies, we found fundamental limits on the broadband performance of quantum sensors. For tasks such as axion detection [42], this implies that spectral sensitivity is a scarce resource that needs to be carefully considered when designing metrological protocols. While conventional spectroscopy protocols such as Ramsey interferometry and CPMG [30, 31] consist only of π-pulses, and therefore linearly accumulate IQFI, we found both continuous and discrete protocols that quadratically increase this accumulation. Moreover, we have shown that this is asymptotically the largest scaling one can achieve.

We see that there are protocols with IQFIs that scale as both $\mathcal{O}(\zeta^2 T)$ and $\mathcal{O}(\zeta^3 BT^2)$, but which is better? It depends—if the goal is sensitivity to a wide range of frequencies, $\mathcal{O}(\zeta^3 BT^2)$ may allow the protocol to work over a wider frequency band. If the goal is sensitivity to a very narrow frequency range, $\mathcal{O}(\zeta^2 T)$ protocols may have support over a small band. Thus, we may see enhancements when searching for a weak signal over a wide frequency range. In such a setting, long integration times could give a quadratic enhancement of the accumulated QFI compared to the $\mathcal{O}(\zeta^2 T)$ protocols.

The gX protocol is sensitive to frequencies around $2g$, making it an excellent candidate for broadband detection around a particular frequency. It is an open question how to design optimal metrological protocols with sensitivity spread evenly over wide bands. Techniques like GRAPE[43] may be useful for this task[44].

Many dynamical decoupling protocols consist solely of π-pulses (e.g., [45]). Such techniques may be described by Eq. 3. Consequently, our results show these decoupling strategies are fundamentally limited - while they can move noise sensitivity, they cannot remove it. We leave open whether such bounds apply to arbitrary protocols.

Our key conceptual contribution is the idea that IQFI is a useful metric for understanding the trade-offs inherent in broadband sensing. In some cases, this metric provides a conservation law that can be summarized by the slogan "no free QFI". In particular, in the case where the interaction picture operator being sensed ($Z_I(t)$) commutes with itself at all times and in the small signal limit ($\zeta BT \to 0$) we showed that QFI at one frequency ultimately comes at the cost of less QFI at another frequency. This is also true for sequences consisting only of π pulses, when the sensor state begins on the equator. Moreover we have also shown that for any protocol there is a limited amount of IQFI that can be accumulated. This demonstrates that while broadband sensing is possible, there is an upper limit on how wide the bandwidth of a given protocol can be if one desires a certain sensitivity. We do not currently know if other classes of control protocols yield strict conservation laws, and we leave this to future work.

The bounds on IQFI that we have found concern single qubit initial states, which can be extended, via Eq. (19), to arbitrary separable states due to QFI's additivity and convexity. As Eq. (19) applies only to separable probe states, we can think of it as a kind of standard quantum limit that cannot be exceeded without entanglement. Indeed, we see that an n-qubit cat state can significantly exceed the $2\pi n\zeta^2 T$ performance of unentangled π-pulse-based protocols. This points to the possibility of using IQFI as a form of entanglement witness, so that the quantum Fisher information at any particular frequency may be consistent with a separable state but the breadth of such sensitivity can only be explained by an entangled state. Mapping out the corresponding Heisenberg limits on multiqubit entangled probes remains an open question. Finally, another interesting open question is if other transformations of QFI spectra might generate new insights into broadband sensing limitations.

Acknowledgments— JLB thanks Simon Jäger for helpful discussions. DH acknowledges helpful discussions with Carl Caves. This work was supported by the NSF JILA PFC grant 1734006. AMP acknowledges funding from a NASA Space Technology Graduate Research Opportunity award.

[1] V. Giovannetti, "Quantum-enhanced measurements: Beating the standard quantum limit," Science **306**, 1330–1336 (2004).
[2] K. M. Backes, D. A. Palken, S. Al Kenany, B. M. Brubaker, S. B. Cahn, A. Droster, Gene C. Hilton, Sumita Ghosh, H. Jackson, S. K. Lamoreaux, and et al., "A quantum enhanced search for dark matter axions," Nature **590**, 238–242 (2021).
[3] W. Wasilewski, K. Jensen, H. Krauter, J. J. Renema, M. V. Balabas, and E. S. Polzik, "Quantum noise limited and entanglement-assisted magnetometry," Phys. Rev. Lett. **104**, 133601 (2010).
[4] Ian D. Leroux, Monika H. Schleier-Smith, and Vladan Vuletić, "Orientation-dependent entanglement lifetime in a squeezed atomic clock," Phys. Rev. Lett. **104**, 250801 (2010).
[5] Benjamin K. Malia, Julián Martínez-Rincón, Yunfan Wu, Onur Hosten, and Mark A. Kasevich, "Free space ramsey spectroscopy in rubidium with noise below the quantum projection limit," Phys. Rev. Lett. **125**, 043202 (2020).
[6] Graham P. Greve, Chengyi Luo, Baochen Wu, and James K. Thompson, "Entanglement-enhanced matter-wave interferometry in a high-finesse cavity," (2021), arXiv:2110.14027 [quant-ph].

[7] Dietrich Leibfried, Emanuel Knill, Signe Seidelin, Joe Britton, R Brad Blakestad, John Chiaverini, David B Hume, Wayne M Itano, John D Jost, Christopher Langer, *et al.*, "Creation of a six-atom 'schrödinger cat' state," Nature **438**, 639–642 (2005).

[8] Thomas Monz, Philipp Schindler, Julio T. Barreiro, Michael Chwalla, Daniel Nigg, William A. Coish, Maximilian Harlander, Wolfgang Hänsel, Markus Hennrich, and Rainer Blatt, "14-qubit entanglement: Creation and coherence," Phys. Rev. Lett. **106**, 130506 (2011).

[9] B. J. Lawrie, P. D. Lett, A. M. Marino, and R. C. Pooser, "Quantum sensing with squeezed light," ACS Photonics **6**, 1307–1318 (2019).

[10] R. C. Pooser, N. Savino, E. Batson, J. L. Beckey, J. Garcia, and B. J. Lawrie, "Truncated nonlinear interferometry for quantum-enhanced atomic force microscopy," Phys. Rev. Lett. **124**, 230504 (2020).

[11] Carlton M. Caves, "Quantum-mechanical noise in an interferometer," Phys. Rev. D **23**, 1693–1708 (1981).

[12] C.W. Helstrom, "Minimum mean-squared error of estimates in quantum statistics," Physics Letters A **25**, 101–102 (1967).

[13] Akio Fujiwara and Hiroshi Nagaoka, "Quantum fisher metric and estimation for pure state models," Physics Letters A **201**, 119–124 (1995).

[14] Samuel L Braunstein and Carlton M Caves, "Statistical distance and the geometry of quantum states," Physical Review Letters **72**, 3439 (1994).

[15] Joshua M Weiner, Kevin C Cox, Justin G Bohnet, Zilong Chen, and James K Thompson, "Superradiant raman laser magnetometer," Applied Physics Letters **101**, 261107 (2012).

[16] Lukas J. Fiderer, Julien M. E. Fraïsse, and Daniel Braun, "Maximal quantum fisher information for mixed states," Phys. Rev. Lett. **123**, 250502 (2019).

[17] J Clarke and I Braginski, "Alex, eds.,"the squid handbook", vol. 1," (2004).

[18] Dmitry Budker and Michael Romalis, "Optical magnetometry," Nature physics **3**, 227–234 (2007).

[19] HB Dang, Adam C Maloof, and Michael V Romalis, "Ultrahigh sensitivity magnetic field and magnetization measurements with an atomic magnetometer," Applied Physics Letters **97**, 151110 (2010).

[20] CL Degen, "Scanning magnetic field microscope with a diamond single-spin sensor," Applied Physics Letters **92**, 243111 (2008).

[21] Olivier Arcizet, Vincent Jacques, Alessandro Siria, Philippe Poncharal, Pascal Vincent, and Signe Seidelin, "A single nitrogen-vacancy defect coupled to a nanomechanical oscillator," Nature Physics **7**, 879–883 (2011).

[22] Shimon Kolkowitz, Ania C Bleszynski Jayich, Quirin P Unterreithmeier, Steven D Bennett, Peter Rabl, JGE Harris, and Mikhail D Lukin, "Coherent sensing of a mechanical resonator with a single-spin qubit," Science **335**, 1603–1606 (2012).

[23] Mustafa Bal, Chunqing Deng, Jean-Luc Orgiazzi, FR Ong, and Adrian Lupascu, "Ultrasensitive magnetic field detection using a single artificial atom," Nature communications **3**, 1–8 (2012).

[24] William D Phillips, William E Cooke, and Daniel Kleppner, "Magnetic moment of the proton in h2o in bohr magnetons," Metrologia **13**, 179 (1977).

[25] Lorenza Viola, Emanuel Knill, and Seth Lloyd, "Dynamical decoupling of open quantum systems," Physical Review Letters **82**, 2417 (1999).

[26] Lorenza Viola and Emanuel Knill, "Robust dynamical decoupling of quantum systems with bounded controls," Physical Review Letters **90**, 037901 (2003).

[27] Kaveh Khodjasteh and Lorenza Viola, "Dynamical quantum error correction of unitary operations with bounded controls," Physical Review A **80**, 032314 (2009).

[28] Lea F Santos and Lorenza Viola, "Enhanced convergence and robust performance of randomized dynamical decoupling," Physical review letters **97**, 150501 (2006).

[29] Jonas Bylander, Simon Gustavsson, Fei Yan, Fumiki Yoshihara, Khalil Harrabi, George Fitch, David G. Cory, Yasunobu Nakamura, Jaw-Shen Tsai, and William D. Oliver, "Noise spectroscopy through dynamical decoupling with a superconducting flux qubit," Nature Physics **7**, 565–570 (2011).

[30] Saul Meiboom and David Gill, "Modified spin-echo method for measuring nuclear relaxation times," Review of scientific instruments **29**, 688–691 (1958).

[31] Herman Y Carr and Edward M Purcell, "Effects of diffusion on free precession in nuclear magnetic resonance experiments," Physical review **94**, 630 (1954).

[32] Łukasz Cywiński, Roman M. Lutchyn, Cody P. Nave, and S. Das Sarma, "How to enhance dephasing time in superconducting qubits," Phys. Rev. B **77**, 174509 (2008).

[33] Mankei Tsang, Howard M. Wiseman, and Carlton M. Caves, "Fundamental quantum limit to waveform estimation," Physical Review Letters **106** (2011), 10.1103/physrevlett.106.090401.

[34] Shengshi Pang and Andrew N. Jordan, "Optimal adaptive control for quantum metrology with time-dependent hamiltonians," Nature Communications **8** (2017), 10.1038/ncomms14695.

[35] Note that the integral in Eq. 6 always exists since the QFI is bounded and asymptotically we have $J(\rho_\omega) \sim (\sum_{i=0}^{N-1} \Theta_i)^2 \sim 1/\omega^2$..

[36] MJ Holland and K Burnett, "Interferometric detection of optical phase shifts at the heisenberg limit," Physical review letters **71**, 1355 (1993).

[37] John J Bollinger, Wayne M Itano, David J Wineland, and Daniel J Heinzen, "Optimal frequency measurements with maximally correlated states," Physical Review A **54**, R4649 (1996).

[38] Leslie Allen and Joseph H Eberly, *Optical resonance and two-level atoms*, Vol. 28 (Courier Corporation, 1987).

[39] Zilong Chen, Justin G. Bohnet, Joshua M. Weiner, and James K. Thompson, "General formalism for evaluating the impact of phase noise on bloch vector rotations," Phys. Rev. A **86**, 032313 (2012).

[40] David Poulin, Angie Qarry, Rolando Somma, and Frank Verstraete, "Quantum simulation of time-dependent hamiltonians and the convenient illusion of hilbert space," Physical review letters **106**, 170501 (2011).

[41] J Huyghebaert and H De Raedt, "Product formula methods for time-dependent schrodinger problems," Journal of Physics A: Mathematical and General **23**, 5777–5793 (1990).

[42] Dmitry Budker, Peter W. Graham, Micah Ledbetter, Surjeet Rajendran, and Alexander O. Sushkov, "Proposal for a cosmic axion spin precession experiment (casper)," Physical Review X **4** (2014), 10.1103/physrevx.4.021030.

[43] Navin Khaneja, Timo Reiss, Cindie Kehlet, Thomas

Schulte-Herbrüggen, and Steffen J. Glaser, "Optimal control of coupled spin dynamics: design of NMR pulse sequences by gradient ascent algorithms," Journal of Magnetic Resonance **172**, 296–305 (2005).

[44] Jing Liu and Haidong Yuan, "Quantum parameter estimation with optimal control," Physical Review A **96** (2017), 10.1103/physreva.96.012117.

[45] Götz S. Uhrig, "Keeping a quantum bit alive by optimized π-pulse sequences," Phys. Rev. Lett. **98**, 100504 (2007).

In these appendices, we provide detailed calculations of the bounds presented in the main text.

A. Derivation of Average IQFI for Instantaneous π-Pulses

Here, we consider a discrete protocol in which a qubit is subject to a series of π-pulses interleaved with free-evolution. After N pulses, the qubit state is given by

$$|\psi(t_N)\rangle = XU(t_N,t_{N-1})XU(t_{N-1},t_{N-2})X....XU(t_1,t_0)|\psi(0)\rangle, \tag{A1}$$

where $|\psi(0)\rangle = \cos\frac{\alpha}{2}|0\rangle + e^{i\beta}\sin\frac{\alpha}{2}|1\rangle$, and $U(t_{i+1},t_i) = e^{-i\mu B\theta(t_{i+1},t_i)Z}$, and

$$\theta(t_{i+1},t_i) := \frac{\sin(\omega t_{i+1}) - \sin(\omega t_i)}{\hbar\omega}. \tag{A2}$$

We commute all the π-pulses through the free-evolution operators, which conjugates every other Z operator, (i.e. $XZX = -Z$). Then all the time-evolution operators commute and can be combined to give,

$$|\psi(t_N)\rangle = X^N \exp[-i\mu B\sum_{n=0}^{N}(-)^n\theta(t_{n+1},t_n)Z]|\psi(0)\rangle. \tag{A3}$$

The QFI can now be directly calculated to be

$$J(\omega) = \frac{4\zeta^2\sin^2\alpha}{\omega^2}\left(\sin(\omega t_0) + 2\left(\sum_{i=1}^{N-1}(-1)^i\sin(\omega t_i)\right) + (-1)^N\sin(\omega t_N)\right)^2. \tag{A4}$$

Expanding the square and combining like terms, one finds

$$J(\omega) = \frac{4\zeta^2\sin^2\alpha}{\omega^2}(\sin^2\omega t_0 + 4\sum_{i=1}^{N-1}(-1)^i\sin\omega t_0\sin(\omega t_i) + 2(-1)^N\sin\omega t_0\sin\omega t_N \tag{A5}$$

$$+ 4(-1)^N\sum_{i=1}^{N-1}(-1)^i\sin\omega t_i\sin(\omega t_N) + \sin^2\omega t_N + 4\left(\sum_{i=1}^{N-1}\sum_{j=1}^{N-1}(-1)^{i+j}\sin\omega t_i\sin(\omega t_j)\right)). \tag{A6}$$

Although quite messy, we are only interested in the integral of this expression over frequency. Taking this integral simplifies things considerably. First, recall that

$$\int_0^\infty \frac{\sin\omega t_i\sin\omega t_j}{\omega^2} = \frac{\pi}{2}\min\{t_i,t_j\}. \tag{A7}$$

Repeated application of this integral yields

$$K(t_N) = \int_0^\infty J(\omega)d\omega = 4\zeta^2\sin^2\alpha(\frac{\pi}{2}t_0 + (-1)^N\pi t_0 + \frac{\pi}{2}t_n + 2\pi t_0\sum_{i=1}^{N-1}(-1)^i \tag{A8}$$

$$+ 2\pi(-1)^N\sum_{i=1}^{N-1}(-1)^i t_i + 2\pi\left(\sum_{i=1}^{N-1}\sum_{j=1}^{N-1}(-1)^{i+j}\min\{t_i,t_j\}\right)). \tag{A9}$$

Noting that $\sum_{i=1}^{N-1}(-1)^i = \frac{1}{2}\left((-1)^N+1\right)$ and that the last two sums add up to zero, we obtain

$$K(t_N) = 2\pi\zeta^2(t_N - t_0)\sin^2\alpha. \tag{A10}$$

We can average over input states to find

$$\langle K(t_N)\rangle = \frac{1}{4\pi}\int_0^{2\pi}d\beta\int_0^\pi d\alpha\sin(\alpha)2\pi\zeta^2(t_N-t_0)\sin^2\alpha, \tag{A11}$$

$$\langle K(t_N)\rangle = \frac{4\zeta^2}{3}\pi(t_N - t_0). \tag{A12}$$

Letting $t_N \to T$ and $t_0 \to 0$, we obtain the result from the main text,

$$\langle K(T)\rangle = \frac{4\zeta^2\pi}{3}T. \tag{A13}$$

B. Derivation of the IQFI under the Rotating Wave Approximation

For the protocol governed by the Hamiltonian

$$H(t) = \mu B \cos \omega t Z + \hbar g X = \begin{pmatrix} \mu B \cos \omega t & \hbar g \\ \hbar g & -\mu B \cos \omega t \end{pmatrix}, \tag{B1}$$

one can ask what the behavior of the system is near resonance ($\omega \sim 2g$). In this regime, we can apply the rotating wave approximation (RWA) to the system and still capture the dynamics. Transforming into the interaction frame with respect to $\hbar g X$ yields the RWA Hamiltonian given as

$$H_{\text{RWA}} = \frac{1}{2} \begin{pmatrix} \mu B & \hbar(2g-\omega) \\ \hbar(2g-\omega) & -\mu B \end{pmatrix}, \tag{B2}$$

and the time-evolution operator is $U_{\text{RWA}}(t) = \exp\left(-\frac{i}{\hbar} H_{\text{RWA}} t\right)$. We take $\mu = \hbar = 1$ to simplify the expressions, then add the pre-factors in at the end of the calculation to restore dimensional consistency. Doing so gives a final state of the form

$$|\psi(t)\rangle_{\text{RWA}} = U_{\text{RWA}}(t)|+\rangle, \tag{B3}$$

$$= \begin{pmatrix} \dfrac{\cos\left(\frac{1}{2}t\sqrt{B^2+(\omega-2g)^2}\right) - \frac{i(B+2g-\omega)\sin\left(\frac{1}{2}t\sqrt{B^2+(\omega-2g)^2}\right)}{\sqrt{B^2+(\omega-2g)^2}}}{\sqrt{2}} \\ \dfrac{\cos\left(\frac{1}{2}t\sqrt{B^2+(\omega-2g)^2}\right) + \frac{i(B-2g+\omega)\sin\left(\frac{1}{2}t\sqrt{B^2+(\omega-2g)^2}\right)}{\sqrt{B^2+(\omega-2g)^2}}}{\sqrt{2}} \end{pmatrix}, \tag{B4}$$

$$:= a|0\rangle + b|1\rangle, \tag{B5}$$

where we have identified

$$a = \frac{\cos\left(\frac{1}{2}t\sqrt{B^2+(\omega-2g)^2}\right) - \frac{i(B+2g-\omega)\sin\left(\frac{1}{2}t\sqrt{B^2+(\omega-2g)^2}\right)}{\sqrt{B^2+(\omega-2g)^2}}}{\sqrt{2}}, \tag{B6}$$

$$b = \frac{\cos\left(\frac{1}{2}t\sqrt{B^2+(\omega-2g)^2}\right) + \frac{i(B-2g+\omega)\sin\left(\frac{1}{2}t\sqrt{B^2+(\omega-2g)^2}\right)}{\sqrt{B^2+(\omega-2g)^2}}}{\sqrt{2}}, \tag{B7}$$

for simplicity. Further defining $\partial_B[a] := c$ and $\partial_B[b] := d$ allows the QFI of estimating B from this final state, $J(\omega) = 4\langle \partial_B \psi(t) \,|\, \psi(t)\rangle^2 + 4\langle \partial_B \psi(t) \,|\, \partial_B \psi(t)\rangle$, to be expressed as

$$J(\omega) = 4\left[(c^* a + d^* b)^2 + c^* c + d^* d\right], \tag{B8}$$

$$= \frac{B^2 t^2}{B^2 + (\omega-2g)^2} + \frac{4\sin^2\left(\frac{t\sqrt{B^2+(\omega-2g)^2}}{2}\right)}{(B^2+(\omega-2g)^2)^2} - \frac{t^2 B^2 (\omega-2g)^2}{(B^2+(\omega-2g)^2)^2} \tag{B9}$$

$$+ \frac{2B^2 t(\omega-2g)^2 \sin\left[t\sqrt{B^2+(\omega-2g)^2}\right]}{(B^2+(\omega-2g)^2)^{5/2}} - \frac{B^2(\omega-2g)^2 \sin^2\left[t\sqrt{B^2+(\omega-2g)^2}\right]}{(B^2+(\omega-2g)^2)^3}. \tag{B10}$$

Now, we can attempt to find the anti-derivatives of each term in this lengthy expression. Denoting the IQFI as $K(\omega)$, we find

$$K(\omega) = \frac{1}{2}Bt^2\left(\tan^{-1}\left(\frac{\omega-2g}{B}\right) + \frac{B(\omega-2g)}{(B^2+(\omega-2g)^2)^2}\right) \tag{B11}$$

$$+\int d\omega\left[\frac{4\sin^2\left(\frac{t\sqrt{B^2+(\omega-2g)^2}}{2}\right)}{(B^2+(\omega-2g)^2)^2} + \frac{2B^2t(\omega-2g)^2\sin\left[t\sqrt{B^2+(\omega-2g)^2}\right]}{(B^2+(\omega-2g)^2)^{5/2}} - \frac{B^2(\omega-2g)^2\sin^2\left[t\sqrt{B^2+(\omega-2g)^2}\right]}{(B^2+(\omega-2g)^2)^3}\right], \tag{B12}$$

$$\leqslant t^2\left(\frac{B}{2}\tan^{-1}\left(\frac{\omega-2g}{B}\right) + \frac{B^2(\omega-2g)}{2(B^2+(\omega-2g)^2)^2}\right) \tag{B13}$$

$$+\int d\omega\left[\frac{4}{(B^2+(\omega-2g)^2)^2} + \frac{2B^2t(\omega-2g)^2}{(B^2+(\omega-2g)^2)^{5/2}} - \frac{B^2(\omega-2g)^2}{(B^2+(\omega-2g)^2)^3}\right], \tag{B14}$$

$$K(\omega) = t^2\left(\frac{B}{2}\tan^{-1}\left(\frac{\omega-2g}{B}\right) + \frac{B^2(\omega-2g)}{2(B^2+(\omega-2g)^2)^2}\right) + \mathcal{I}(t), \tag{B15}$$

where we have let $\mathcal{I}(t)$ represent the unwieldy integral. When integrated, the result is at most linear in t. Focusing on the first term, which dominates for $T \gg 1$, we can evaluate the anti-derivative to recover the expression in the main text. The RWA holds in a frequency band around the resonant peak, which we take to be $\omega = g$ to $\omega = 3g$. Evaluating the anti-derivative over this band, we obtain

$$K(T) \gtrsim B\mu T^2\left(\frac{Bg\mu}{B^2\mu^2+g^2} + \tan^{-1}\left(\frac{g}{B\mu}\right)\right). \tag{B16}$$

Restoring dimensional consistency, we obtain the expression from the main text

$$K(T) \gtrsim \zeta^2T^2\left(\frac{g}{1+\frac{g^2}{\zeta^2B^2}} + \zeta B\tan^{-1}\left(\frac{g}{\zeta B}\right)\right). \tag{B17}$$

C. Proof of $\mathcal{O}(T^2)$ IQFI Scaling for Continuous-Time Protocols

1. Bound on IQFI of Continuous Protocols

As in the main text, consider a sensing protocol defined by a time-dependent control $G(T)$. In particular, the full Hamiltonian we are considering is

$$H(T) = \hbar G(T) + \mu B\cos(\omega T)Z. \tag{C1}$$

We can Trotterize the evolution into a discrete sequence [40], which will look like those considered in the proof above, with some step size δt. The evolution will be

$$U'(T) = \mathcal{T}e^{i\int_{(N-1)\delta t}^{N\delta t}dtG(t)}e^{i\zeta B\Theta_N Z}\ldots\mathcal{T}e^{i\int_0^{\delta t}dtG(t)}e^{i\zeta B\Theta_1 Z} + O(\delta t^2) \tag{C2}$$

with $\Theta_k = [\sin(\omega k\delta t) - \sin(\omega(k-1)\delta t)]/(\hbar\omega)$, $N\delta t = T$, and where $\mathcal{T}$ denotes the time-ordering operator, which is necessary because in general $G(t)$ will not commute with itself at all times. The number of pulses, N, in the discrete protocol described in Eq. C2 gives, to zeroth order,

$$\int d\omega J_c(\omega) \leqslant \frac{2\pi\zeta^2T^2}{\delta t}, \tag{C3}$$

for all δt. There are however error terms from the Trotter expansion that we need to propagate through the IQFI - this is what we will do now. By linearity of the derivative operator we can also constrain the derivative of the Trotterized evolution to be close to the derivative of the actual evolution. In particular, we have that

$$U(T) = U'(T) + \hat{\epsilon}'(T) \tag{C4}$$

$$\partial_B U(T) = \partial_B U'(T) + \hat{\epsilon}''(T) \tag{C5}$$

where $\hat{\epsilon}''(T) = \partial_B \hat{\epsilon}'(T)$ is the B derivative of the error term in the Trotter expansion. Then we see from Eq. 23,

$$J_c(\omega) \leqslant J_d(\omega) + 4(\langle +|\hat{\epsilon}''^{\dagger}(T)\partial_B U'(T) + \partial_B U'^{\dagger}(T)\hat{\epsilon}''(T)|+\rangle + \langle +|\hat{\epsilon}''(T)^{\dagger}\hat{\epsilon}''(T)|+\rangle) \tag{C6}$$

$$= J_d(\omega) + 8Re(\langle +|\hat{\epsilon}''(T)^{\dagger}\partial_B U'(T)|+\rangle) + 4\langle +|\hat{\epsilon}''(T)^{\dagger}|\hat{\epsilon}''(T)|+\rangle). \tag{C7}$$

We will analyze the integrals of the error terms piecewise, first up to a frequency $\Omega > 0$. The derivative of the the first order Trotterized evolution defined above is

$$\partial_B U'(T) = -i\zeta \sum_{j=0}^{N-1} \Theta_j P_0 U_0 ... P_j Z U_j ... P_{N-1} U_{N-1}. \tag{C8}$$

Noting that $|\Theta_k| \leqslant 2T/N$ for a uniformly spaced pulse sequence, this gives

$$|| \int_0^{\Omega} \hat{\epsilon}''(T)(-\frac{i\mu}{\hbar}) \sum_{j=0}^{N-1} \Theta_j P_0 U_0 ... P_j U_j ... P_{n-1} U_{n-1}|| \tag{C9}$$

$$\leqslant \frac{\mu}{\hbar} \max_{\omega<\Omega} ||\hat{\epsilon}''(T)|| \int_0^{\Omega} \sum_{j=0}^{N-1} |\Theta_j| ||P_0 U_0 ... P_j U_j ... P_{n-1} U_{n-1}|| \tag{C10}$$

$$\leqslant \frac{\mu}{\hbar} \max_{\omega<\Omega} ||\hat{\epsilon}''(T)|| \int_0^{\Omega} \sum_{j=0}^{N-1} 2T/N \tag{C11}$$

$$= \frac{2\mu}{\hbar} \max_{\omega<\Omega} ||\hat{\epsilon}''(T)|| \Omega T, \tag{C12}$$

Similarly,

$$4 \int_0^{\Omega} ||\hat{\epsilon}''(T)^{\dagger}\hat{\epsilon}''(T)|| \leqslant 4\max_{\omega<\Omega} ||\hat{\epsilon}''(T)||^2 \Omega \tag{C13}$$

where the maximum is over ω on which the error term implicitly depends. Then we have, for the last two terms in Eq. C7

$$8|| \int_0^{\infty} Re(\hat{\epsilon}''^{\dagger}(T)\partial_B U'(T))|| \leqslant \frac{16\mu}{\hbar} \Omega T \max_{\omega<\Omega} ||\hat{\epsilon}''(T)|| + || \int_{\Omega}^{\infty} 8Re(\hat{\epsilon}''^{\dagger}(T)\partial_B U'(T))||, \tag{C14}$$

and

$$4 \int_0^{\infty} ||\hat{\epsilon}''(T)^{\dagger}\hat{\epsilon}''(T)|| \leqslant 4\max_{\omega<\Omega} ||\hat{\epsilon}''(T)||^2 \Omega + 4 \int_{\Omega}^{\infty} ||\hat{\epsilon}''(T)^{\dagger}\hat{\epsilon}''(T)||. \tag{C15}$$

$\hat{\epsilon}''(T)$ is at worst proportional to T, since the error in a time step δt is independent of T (it's proportional to $||[\hbar G(t), \mu B \cos{(\omega t)} Z]|| \delta t^2$), and there are $N = T/\delta t$ times steps. Furthermore

$$||\partial_B U'(T)|| = || \frac{-i\mu}{\hbar} \sum_j \Theta_j P_1 U_1 ... P_j U_j ... P_n U_n || \leqslant \mu N/(\hbar\omega) = \mu T/(\delta t \hbar \omega), \tag{C16}$$

so we need only understand $||\hat{\epsilon}''(T)||$ at high frequency, where $|| \cdot ||$ is the spectral norm. To this end, consider the error in time step δt given in [41] as $U'(t_k, t_{k-1})F(t_k, t_{k-1})$, where $U'(a, b)$ is the Trotterized evolution from time a to time b and

$$F(t_k, t_{k-1}) = \int_{t_{k-1}}^{t_k} C(v, t_{k-1}) F(v, t_{k-1}) dv \tag{C17}$$

$$C(t_k, t_{k-1}) = exp(i \int_{t_{k-1}}^{t_k} G(s)ds)^{\dagger} \int_{t_{k-1}}^{t_k} du \; exp(i \int_{t_{k-1}}^{u} A(s)ds)^{\dagger} \tag{C18}$$

$$\times [A(u), \hbar G(t_k)] exp(-i \int_{t_{k-1}}^{u} A(s)ds) exp(-i \int_{t_{k-1}}^{t_k} G(s)ds), \tag{C19}$$

where $A(s) = \frac{\mu B}{\hbar}\cos(\omega s)Z$. Thus, to lowest order in $1/\omega$,

$$\exp(-i\int_{t_{k-1}}^{u} A(s)ds) = \exp(iBZ(\cos(\omega u) - \cos(\omega t_{k-1}))/\omega) \approx I - i\frac{\mu B}{\hbar}Z(\cos(\omega u) - \cos(\omega t_{k-1}))/\omega \tag{C20}$$

so that the relevant integrals over u are

$$\int_{t_{k-1}}^{t_k} du\cos(\omega u) = (\sin(\omega t_k) - \sin(\omega t_{k-1}))/\omega \tag{C21}$$

$$\int_{t_{k-1}}^{t_k} du\cos(\omega u)(\cos(\omega u) - \cos(\omega t_{k-1})) \tag{C22}$$

$$= (2\delta t\omega + \sin(2t_{k-1}\omega) - 4\cos(t_{k-1}\omega)\sin((t_{k-1}+\delta t)\omega) + \sin(2(t_{k-1}+\delta t)\omega))/(4\omega) \tag{C23}$$

Plugging these in we find

$$C(t_k, t_{k-1}) = \frac{\mu B}{\hbar}((\sin(\omega t_k) - \sin(\omega t_{k-1}))/\omega)(\exp(i\int_{t_{k-1}}^{t_k}\hbar G(s)ds)^{\dagger}[Z, \hbar G(t_k)]\exp(-i\int_{t_{k-1}}^{t_k}\hbar G(s)ds)) \tag{C24}$$

$$+\frac{i2\zeta^2 B^2}{4\omega^2}((2\delta t\omega + \sin(2t_{k-1}\omega) - 4\cos(t_{k-1}\omega)\sin((t_{k-1}+\delta t)\omega) + \sin(2(t_{k-1}+\delta t)\omega)) \tag{C25}$$

$$\times(\exp(i\int_{t_{k-1}}^{t_k}\hbar G(s)ds)^{\dagger} Z[Z, \hbar G(t_k)]\exp(-i\int_{t_{k-1}}^{t_k}\hbar G(s)ds)) \tag{C26}$$

$$+(\exp(i\int_{t_{k-1}}^{t_k}\hbar G(s)ds)^{\dagger}[Z, \hbar G(t_k)]Z\exp(-i\int_{t_{k-1}}^{t_k}\hbar G(s)ds))))), \tag{C27}$$

where we have only kept the lowest order correction terms. By inspection, we see that there is no way for a T dependence to enter for higher order terms, and moreover we see that for ω large enough ($\Omega >> \mu B/\hbar$) the terms are both integrable over ω and arbitrarily small. We are interested in N times the B-derivative of this error, where the extra factor of N is because the total error accumulates at worst as N times the step-wise error. But now we are done, since this shows that for all $\epsilon > 0$ there is an $\Omega(||G||, B, \delta t)$ such that in total we have a bound of

$$\int d\omega J_c(\omega) \leqslant \frac{2\pi\zeta^2 T^2}{\delta t} + (c(\hbar||G||, \mu B, \delta t) + \epsilon(\hbar||G||, \mu B, \delta t))T^2, \tag{C28}$$

where we've denoted two parts in the coefficient of the second term - one coming from the lowest order contribution to the right tail of the QFI, and one coming from the innaccuracy in this approximation. So in total we see that $\int d\omega K(T) \in \mathcal{O}(T^2)$.

D. Perturbative Expansion to $\mathcal{O}(B^2)$

Recall that the pure state QFI can be expressed as

$$J(\rho) = 4\langle\phi|\phi\rangle + 4\text{Re}\{\langle\phi|\psi\rangle^2\}. \tag{D1}$$

As shown in a previous note, the second term above is in general non-positive and thus if all we seek is an upper bound on the QFI, we can simply consider the first term. We can write the time evolution operator as

$$\mathcal{U} = 1 - iB\int_0^t \cos(\omega\tau)Z_I(\tau)d\tau - B^2\int_0^t d\tau_2\int_0^{\tau_2} d\tau_1\cos(\omega\tau_2)\cos(\omega\tau_1)Z_I(\tau_2)Z_I(\tau_1) \tag{D2}$$

$$+ iB^3\int_0^t d\tau_3\int_0^{\tau_3} d\tau_2\int_0^{\tau_2} d\tau_1\cos(\omega\tau_3)\cos(\omega\tau_2)\cos(\omega\tau_1)Z_I(\tau_3)Z_I(\tau_2)Z_I(\tau_1) + \mathcal{O}(B^4), \tag{D3}$$

where we have used $Z_I(t)$ to express Z in the interaction picture. We expand to order B^3 because, when differentiated with respect to B, this yields a term proportional to B^2. To simplify notation, let

$$\mathcal{U} := 1 - iBI_1 - B^2 I_2 + iB^3 I_3 + \mathcal{O}(B^4). \tag{D4}$$

Then, the time-evolved quantum state will be

$$|\psi\rangle := |\psi(t)\rangle = U_0\mathcal{U}|\psi(0)\rangle, \tag{D5}$$

and the derivative of this state is then

$$\begin{aligned}
|\phi\rangle &:= \partial_B|\psi\rangle, && \text{(D6)}\\
&= \partial_B|\psi(t)\rangle, && \text{(D7)}\\
&= \partial_B(U_0\mathcal{U}|\psi(0)\rangle), && \text{(D8)}\\
&= (-iU_0I_1 - 2BU_0I_2 + i3B^2U_0I_3)|\psi(0)\rangle + \mathcal{O}(B^3). && \text{(D9)}
\end{aligned}$$

The inner product of this vector with itself is,

$$\begin{aligned}
\langle\phi|\phi\rangle &= \langle\psi(0)|(+iI_1^\dagger U_0^\dagger - 2BI_2^\dagger U_0^\dagger - i3B^2I_3^\dagger U_0^\dagger)(-iU_0I_1 - 2BU_0I_2 + i3B^2U_0I_3)|\psi(0)\rangle + \mathcal{O}(B^3), && \text{(D10)}\\
&= \langle\psi(0)|I_1^\dagger I_1|\psi(0)\rangle - i2B\langle\psi(0)|I_1^\dagger I_2|\psi(0)\rangle - 3B^2\langle\psi(0)|I_1^\dagger I_3|\psi(0)\rangle + && \text{(D11)}\\
&+ i2B\langle\psi(0)|I_2^\dagger I_1|\psi(0)\rangle + 4B^2\langle\psi(0)|I_2^\dagger I_2|\psi(0)\rangle - 3B^2\langle\psi(0)|I_3^\dagger I_1|\psi(0)\rangle + \mathcal{O}(B^3). && \text{(D12)}\\
& && \text{(D13)}
\end{aligned}$$

Now we assume, and verify later, that $\langle\psi(0)|I_1^\dagger I_2|\psi(0)\rangle = \langle\psi(0)|I_2^\dagger I_1|\psi(0)\rangle$ and $\langle\psi(0)|I_1^\dagger I_3|\psi(0)\rangle = \langle\psi(0)|I_3^\dagger I_1|\psi(0)\rangle$, so we have

$$\langle\phi|\phi\rangle = \langle\psi(0)|I_1^\dagger I_1|\psi(0)\rangle + 4B^2\langle\psi(0)|I_2^\dagger I_2|\psi(0)\rangle - 6B^2\langle\psi(0)|I_1^\dagger I_3|\psi(0)\rangle + \mathcal{O}(B^3). \tag{D14}$$

From our work above, we have $J(\rho) \leqslant 4\langle\phi|\phi\rangle$. Also, because $J(\rho)$ is an even function of ω, $\int_{-\infty}^{\infty} J(\rho)d\omega = 2\int_0^\infty J(\rho)d\omega := 2J_{\text{tot}}$. Thus,

$$\begin{aligned}
J_{\text{tot}} &= \frac{1}{2}\int_{-\infty}^{\infty} J(\rho)d\omega, && \text{(D15)}\\
&\leqslant \frac{1}{2}\int_{-\infty}^{\infty} 4\langle\phi|\phi\rangle d\omega, && \text{(D16)}\\
&= 2\int_{-\infty}^{\infty}\langle\phi|\phi\rangle d\omega. && \text{(D17)}
\end{aligned}$$

Thus, our task has become integrating Eq. D14 over all frequencies. Let's start with the first term, which we write out explicitly because the same technique will be applied to the other terms. We have

$$\begin{aligned}
& 2\int_{-\infty}^{\infty}\langle\psi(0)|I_1^\dagger I_1|\psi(0)\rangle d\omega && \text{(D18)}\\
&= 2\int_{-\infty}^{\infty}\langle\psi(0)|\left(\int_0^{t'} d\tau'\cos(\omega\tau')Z_I(\tau')\right)\left(\int_0^{t} d\tau\cos(\omega\tau)Z_I(\tau)\right)|\psi(0)\rangle d\omega, && \text{(D19)}\\
&= 2\int_{-\infty}^{\infty}\langle\psi(0)|\left(\int_0^{t'} d\tau'\int_0^{t} d\tau\cos(\omega\tau')\cos(\omega\tau)Z_I(\tau')Z_I(\tau)\right)|\psi(0)\rangle d\omega. && \text{(D20)}\\
& && \text{(D21)}
\end{aligned}$$

Now, let us note the following useful fact,

$$2\pi\delta(\tau' - \tau) = \int_{-\infty}^{\infty} e^{i\omega(\tau'-\tau)}d\omega. \tag{D22}$$

With this in mind, we can write

$$2\int_{-\infty}^{\infty}\langle\psi(0)|I_1^\dagger I_1|\psi(0)\rangle d\omega \tag{D23}$$

$$= 2\int_{-\infty}^{\infty}\langle\psi(0)|\left(\int_0^{t'} d\tau'\int_0^t d\tau\left(\frac{\cos\omega(\tau'-\tau)+\cos\omega(\tau'+\tau)}{2}\right)Z_I(\tau')Z_I(\tau)\right)|\psi(0)\rangle d\omega \tag{D24}$$

$$= \frac{1}{2}\int_{-\infty}^{\infty}\langle\psi(0)|\left(\int_0^{t'} d\tau'\int_0^t d\tau\left(e^{i\omega(\tau'-\tau)}+e^{-i\omega(\tau'-\tau)}+e^{i\omega(\tau'+\tau)}+e^{-i\omega(\tau'+\tau)}\right)Z_I(\tau')Z_I(\tau)\right)|\psi(0)\rangle d\omega \tag{D25}$$

$$= \pi\langle\psi(0)|\left(\int_0^{t'} d\tau'\int_0^t d\tau\left[\delta(\tau'-\tau)+\delta(-(\tau'-\tau))+\delta(\tau'+\tau)+\delta(-(\tau'+\tau))\right]Z_I(\tau')Z_I(\tau)\right)|\psi(0)\rangle \tag{D26}$$

$$= \pi\langle\psi(0)|\left(\int_0^{t'} d\tau'\int_0^t d\tau 2\delta(\tau'-\tau)Z_I(\tau')Z_I(\tau)\right)|\psi(0)\rangle \tag{D27}$$

$$= 2\pi\int_0^{t'} d\tau'\langle\psi(0)|Z_I(\tau')Z_I(\tau')|\psi(0)\rangle \tag{D28}$$

$$= 2\pi\int_0^{t'} d\tau'\langle\psi(0)\,|\,\psi(0)\rangle \tag{D29}$$

$$= 2\pi\int_0^{t'} d\tau' \tag{D30}$$

$$= 2\pi t', \tag{D31}$$

where we have used the facts that $\delta(-x)=\delta(x)$, the delta functions $\delta(\tau'+\tau)=0$ for the range over which we are integrating, $Z_I(\tau')Z_I(\tau')=\mathbb{I}$, and $\langle\psi(0)\,|\,\psi(0)\rangle=1$. Next, we turn to the second term in Eq. D14. We have

$$8B^2\int_{-\infty}^{\infty}\langle\psi(0)|I_2^\dagger I_2|\psi(0)\rangle d\omega \tag{D32}$$

$$= 8B^2\int_{-\infty}^{\infty}\langle\psi(0)|\left(\int_0^{t'} d\tau_2'\int_0^{\tau_2'} d\tau_1'\cos(\omega\tau_2')\cos(\omega\tau_1')Z_I(\tau_2')Z_I(\tau_1')\right) \tag{D33}$$

$$\times\left(\int_0^t d\tau_2\int_0^{\tau_2} d\tau_1\cos(\omega\tau_2)\cos(\omega\tau_1)Z_I(\tau_2)Z_I(\tau_1)\right)|\psi(0)\rangle d\omega, \tag{D34}$$

$$= 8B^2\int_{-\infty}^{\infty}\langle\psi(0)|\left(\int_0^{t'} d\tau_2'\int_0^{\tau_2'} d\tau_1'\int_0^t d\tau_2\int_0^{\tau_2} d\tau_1\prod_i\cos(\omega\tau_i)Z_I(\tau_i)\right)|\psi(0)\rangle d\omega, \tag{D35}$$

(D36)

where we have abused notation in attempt to compactly express the product of cosines and Z_I's. As above, the integral over all frequencies kills one of the time integrals, leaving three. Finally, bounding the expectation value of the product of Z_I's from above by 1, we have

$$8B^2\int_{-\infty}^{\infty}\langle\psi(0)|I_2^\dagger I_2|\psi(0)\rangle d\omega \leqslant 16\pi B^2 t^3. \tag{D37}$$

Similarly, for the last term we have

$$12B^2\int_{-\infty}^{\infty}\langle\psi(0)|I_1^\dagger I_3|\psi(0)\rangle d\omega \leqslant 24\pi B^2 t^3. \tag{D38}$$

Together, this yields an upper bound on the IQFI of

$$J_{\text{tot}} \leqslant 2\pi t + 40\pi B^2 t^3 + \mathcal{O}(B^3) \tag{D39}$$